Robotics and Computer-Integrated Manufacturing 27 (2011) 115–123

Contents lists available at ScienceDirect

Robotics and Computer-Integrated Manufacturing

journal homepage: www.elsevier.com/locate/rcim

Fault detection on robot manipulators using artificial neural networks

Ikbal Eski, Selcuk Erkaya, Sertaç Savas, Sahin Yildirim *

Erciyes University, Engineering Faculty, Mechatronics Engineering Department, Kayseri 38039, Turkey

ARTICLE INFO

Article history:
Received 1 February 2010
Received in revised form
17 June 2010
Accepted 23 June 2010

Keywords:
Fault detection
Neural network
Robot manipulator
Vibration analysis

ABSTRACT

Nowadays, gas welding applications on vehicle's parts with robot manipulators have increased in automobile industry. Therefore, the speed of end-effectors of robot manipulator is affected on each joint during the welding process with complex trajectory. For that reason, it is necessary to analyze the noise and vibration of robot's joints for predicting faults. This paper presents an experimental investigation on a robot manipulator, using neural network for analyzing the vibration condition on joints. Firstly, robot manipulator's joints are tested with prescribed of trajectory end-effectors for the different joints speeds. Furthermore, noise and vibration of each joint are measured. And then, the related parameters are tested with neural network predictor to predict servicing period. In order to find robust and adaptive neural network structure, two types of neural predictors are employed in this investigation. The results of two approaches improved that an RBNN type can be employed to predict the vibrations on industrial robots.

1. Introduction

Recently, different fault detection, fault diagnoses, fault detection and isolation, fault identification, fault-tolerance, etc. techniques for robot manipulators have been proposed in the literature. Some of important survey papers have been presented for these techniques for robot manipulators. Caccavale et al. were proposed a fault diagnosis approach for robotic manipulators, subject to faults of the joints driving systems. A model-based diagnostic observer was adopted to detect, isolate and identify failures. The effectiveness of the approach was experimentally tested on an industrial robot manipulator [1]. Halder and Sarkar were presented a new robust nonlinear analytic redundancy technique to actuator fault detection for input-affine nonlinear multivariable dynamic systems. Experimental results on a PUMA 560 robotic arm were presented to demonstrate the application of the theorem [2].

Moreover the joint velocity jump during fault tolerant operations for redundant manipulators was defined, and the analytical formulation of joint velocity of the reduced manipulator with minimum joint velocity jump was derived by Jing and Cheng [3]. Two fault-tolerant control strategies for robot manipulators were researched by Siqueira et al. These strategies were implemented based on output-feedback $H\infty$ controllers, and experimental results of each controller were given [4]. Hassan and Notash were presented a methodology to modify the kinematic layout of parallel manipulators to provide fault-tolerance to active-joint jam at a large number of end-effector poses. The optimization procedure was applied successfully on a 6-degree of freedom example manipulator [5]. Similarly, modification of parallel manipulators to achieve fault-tolerance to active-joint jam was performed by equipping each branch with a backup revolute joint at a pre-assigned location [6]. Another study, problem of fault-tolerance in cooperative manipulators rigidly connected to a load was investigated [7].

In order to stabilize the reinforcement-learning environment, Yasuda and Ohkura were used a neural network for predicting the average of the other robots' postures at the next time step. Computer simulations were conducted to illustrate the fault-tolerance of our MRS against a system change that occurs after the MRS achieves stable behavior [8]. Verma and Simmons were presented a new algorithm for computationally tractable fault diagnosis. Experiments with a dynamic simulation of a six-wheel rocker-bogie rover showed a significant improvement in performance over the classical approach [9]. Fault tolerant motion planning of two spatial coordinating manipulators having two possible locked joints, respectively, was researched. Simulation result for two spatial 4R manipulators was demonstrated the validity of this proposed algorithm [10].

Another investigation, Notash and Huang presented methodologies for the design of fault tolerant parallel manipulators based on the failure analysis of manipulators and optimum fault tolerant configuration of each class was identified [11]. A strategy of fault tolerant tripod gait was proposed by Yang and a periodic gait was presented, in which hexapod walking machines have the maximum stride length after a locked failure. The adjustment procedure from a normal gait to the proposed fault tolerant gait was shown to demonstrate the applicability of the proposed scheme [12].

* Corresponding author. Tel.: +90 0352 4374901 32053; fax: +90 0 352 4375784.
E-mail address: sahiny@erciyes.edu.tr (S. Yildirim).

0736-5845/$ - see front matter Crown Copyright © 2010 Published by Elsevier Ltd. All rights reserved.
doi:10.1016/j.rcim.2010.06.017

Nomenclature

b	best matching unit
b_j	bias of the jth neuron in the hidden layer
b_k	bias of the kth neurons in the output layer
c_j	corresponding coefficient
$f(t)$	activation function of the hidden layer
$F(\dot{\boldsymbol{q}}(t))$	friction term of robot manipulator's joints
$\boldsymbol{F_v(t)}$	diagonal matrix of viscous friction coefficients
$g(t)$	activation functions of the output layer
$\boldsymbol{G(q(t))}$	vector of gravity terms
$h_{bi}(t)$	neighborhood kernel centered on the winner unit
$h_{bj}(t)$	neighborhood kernel centered at unit b
K_{dn}	the coefficients of dynamic friction
m	total number of terms in the polynomial
$m_j(t)$	output function of the jth neuron in the hidden layer
M	number of map unit
$\boldsymbol{M(q(t))}$	inertia matrix of the robot manipulator
N	number of training samples
n_I	number of neurons in the input layer
n_H	number of neurons in the hidden layer
n_O	number of neurons in the output layer
r_b	position of neurons b on the SOMNN grid
r_i	position of neurons i on the SOMNN grid
$RBNN$	radial basis neural network
$sgn(\dot{q}_n)$	the signum function
$SOMNN$	self organizing map neural network
$\boldsymbol{V_m}(q(t),\dot{\boldsymbol{q}}(t))$	vector of centrifugal and Coriolis terms
w_{ij}	weight of the connection between the input and hidden layer neurons
w_{jk}	weight of the connection between the hidden and output layer neurons
$\boldsymbol{x}$	vector of input variables
x_i	center of basis function ϕ
y_i	acceleration output of the joint i
$\boldsymbol{z_i}$	the best matching unit of vector
$\tau_d(t)$	disturbances
$\boldsymbol{\tau(t)}$	control input vector
$\alpha(t)$	adaptation coefficient
γ	momentum term

The sudden change of joint velocity in fault tolerant operations for two coordinating manipulators has been investigated by Jing et al. A performance criterion with the sudden change in joint velocity and corresponding fault tolerant planning algorithm was presented [13]. Liu and Coghill were presented a model-based approach to an online robotic fault diagnosis and simulation results were presented in their paper [14].

In this paper, two types of neural network predictors are used to detect actuator faults on 6° of industrial robot manipulator. The paper is organized as follows: Section 2 describes the theory of robot manipulators. Section 3 gives some details about neural networks and the proposed neural network predictor. The experimental and simulation investigation's results are given in Section 4. Finally, this paper is concluded with conclusions and discussion in Section 5.

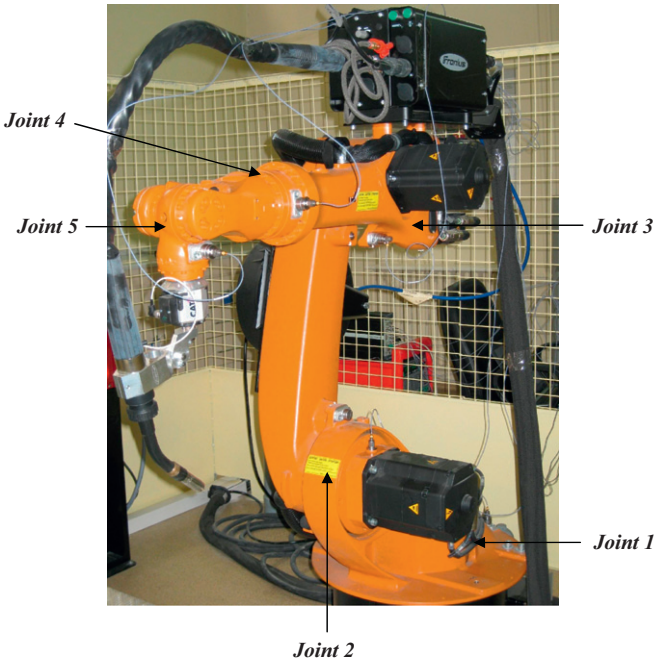

Fig. 1. Experimental system setup with measuring joints.

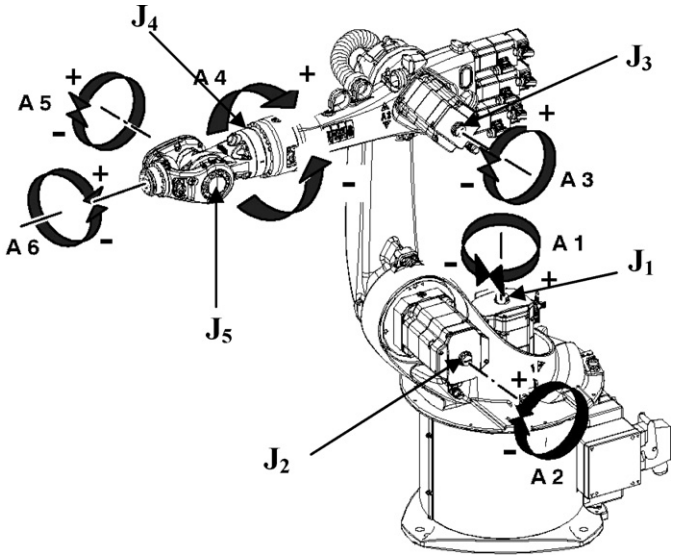

Fig. 2. Schematic joints rotations description of the welding robot manipulator.

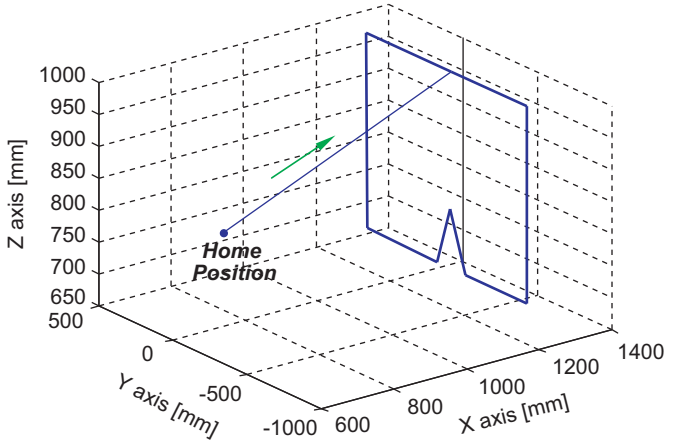

Fig. 3. Trajectory of end-effectors.

2. Representation of welding robot manipulator

The robots described are six-axis industrial robots with jointed-arm kinematics for all point-to-point and continuous-path controlled tasks. Their main areas of application are: (i) handling, (ii) assembly, (iii) application of adhesives, sealants and preservatives, (iv) machining. This robot has six degrees of freedom. It is employed to analyze the vibration parameters of joints as shown in Figs. 1 and 2. The robot manipulator's joints are driven by electromechanical, with transistor controlled AC servo motors. Maximum speed of robot manipulator's end-effectors is 6000 mm/s. The positioning repetition accuracy of the robot manipulator is × 0.1 mm. The trajectory of end-effectors is given in Fig. 3 and the axis properties for the investigated robot manipulator are given in Table 1. The dynamics of robot manipulator with five rigid links can be written as

$$M(q(t))\ddot{\mathbf{q}}(t)+\mathbf{V_m}(q(t),\dot{\mathbf{q}}(t))\dot{\mathbf{q}}(t)+F(\dot{\mathbf{q}}(t))+G(q(t))+\boldsymbol{\tau}_\mathbf{d}(t)=\boldsymbol{\tau}(t) \quad (1)$$

where $\boldsymbol{M(q(t))}$ is then $n\times n$ inertia matrix of the robot manipulator, $\boldsymbol{V_m}(q(t),\dot{\boldsymbol{q}}(t))$ is the $n\times 1$ vector of centrifugal and Coriolis terms, $F(\dot{\boldsymbol{q}}(t))$ is the $n\times n$ friction term, $\boldsymbol{G(q(t))}$ is $n\times 1$ the vector of gravity terms and $\boldsymbol{\tau_d(t)}$ $n\times 1$ represents disturbances ($n=6$). The control input vector $\boldsymbol{\tau(t)}$ has $n\times 1$ components of torque for revolute joints and force for prismatic joints. It is often convenient to write the robot manipulator nonlinear dynamics as

$$M(q(t))\ddot{\mathbf{q}}(t)+N(q(t),\dot{\mathbf{q}}(t))+\boldsymbol{\tau}_\mathbf{d}(t)=\boldsymbol{\tau}(t) \quad (2)$$

where

$$N(q(t),\dot{\mathbf{q}}(t))\equiv\mathbf{V_m}(q(t),\dot{\mathbf{q}}(t))\dot{\mathbf{q}}(t)+F(\dot{\mathbf{q}}(t))+G(q(t)) \quad (3)$$

represents a vector of the nonlinear terms. As depicted from Eq. (3), the joints of robot manipulator are affected by friction terms. These terms can be described;

$$F(\dot{\mathbf{q}}(t))=\mathbf{F_v}(t)\mathbf{q}(t)+\mathbf{F_d}((\mathbf{q}(t)) \quad (4)$$

with $\boldsymbol{F_v(t)}$, a diagonal matrix of constant coefficients representing the viscous friction and $\boldsymbol{F_d}((\dot{\boldsymbol{q}}(t))$ a vector with entries like $K_{\mathrm{dn}}sgn(\dot{q}_n)$ with $sgn(\dot{q}_n)$ the signum function and K_{dn} the coefficients of dynamic friction.

Table 1
Kinematic parameter variations of the welding robot manipulator joints.

Axis	Range of motion	Speed
1	±185°	156°/s
2	+35° to −155°	156°/s
3	+154° to −130°	156°/s
4	±350°	343°/s
5	±130°	362°/s
6	±350°	659°/s

2.1. Structure of the welding robot manipulator controller

The welding robot manipulator controller has some properties as follows:

- Performance and expansion over and above the basic control functions.
- Open system for future developments and ease of integration in any network.
- Recognized standards.
- Special functions for increased productivity.
- Built-in safety features for greater availability.
- Input functions for faster programming.
- Ready-made software packages and real-time capable simulations.
- Offline programs with absolutely accurate data.

The welding robot manipulator controller consists of four components. These

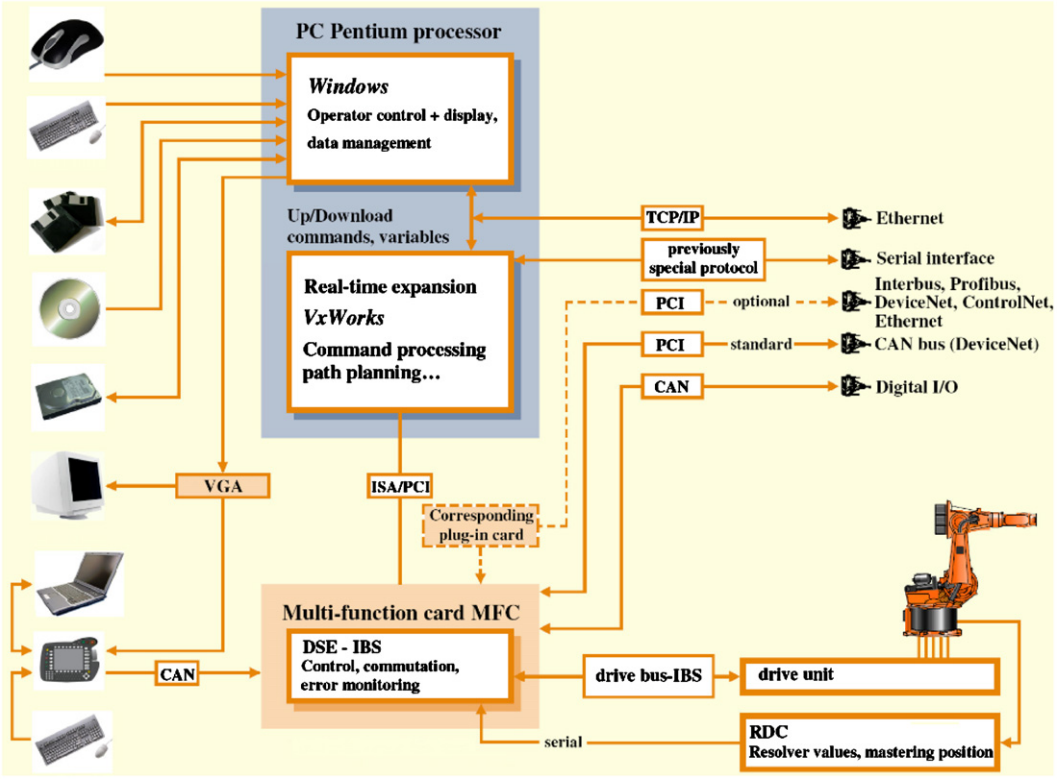

Fig. 4. The welding robot manipulator controller hardware structure.

Control PC: the PC performs all the functions of the robot controller. The control PC includes the following components: motherboard with interfaces, processor and main memory, hard drive, floppy disk drive, CD-ROM drive, MFC3, KVGA, DSE-IBS-C33, batteries and bus cards.
Teach pendant: the teach pendant has all the functions required for operating and programming the robot system.
Safety logic and power unit: the safety logic is a dual-channel computer aided safety system. It permanently monitors all connected safety-relevant components. In the event of a fault or interruption in the safety circuit, the power supply to the drives is shut off, thus bringing the robot system to a standstill.

The hardware of the system is a single processor basis. With a latest generation high-performance processor for two parallel operates systems. The controller hardware structure of the system is shown in Fig. 4.

3. The proposed neural network

Feedforward neural network with three layered is used to analyze acceleration of the welding robot manipulator's joints in this study. Schematic representations of an RBNN and SOMNN analyzers are shown in Fig. 5a and b.

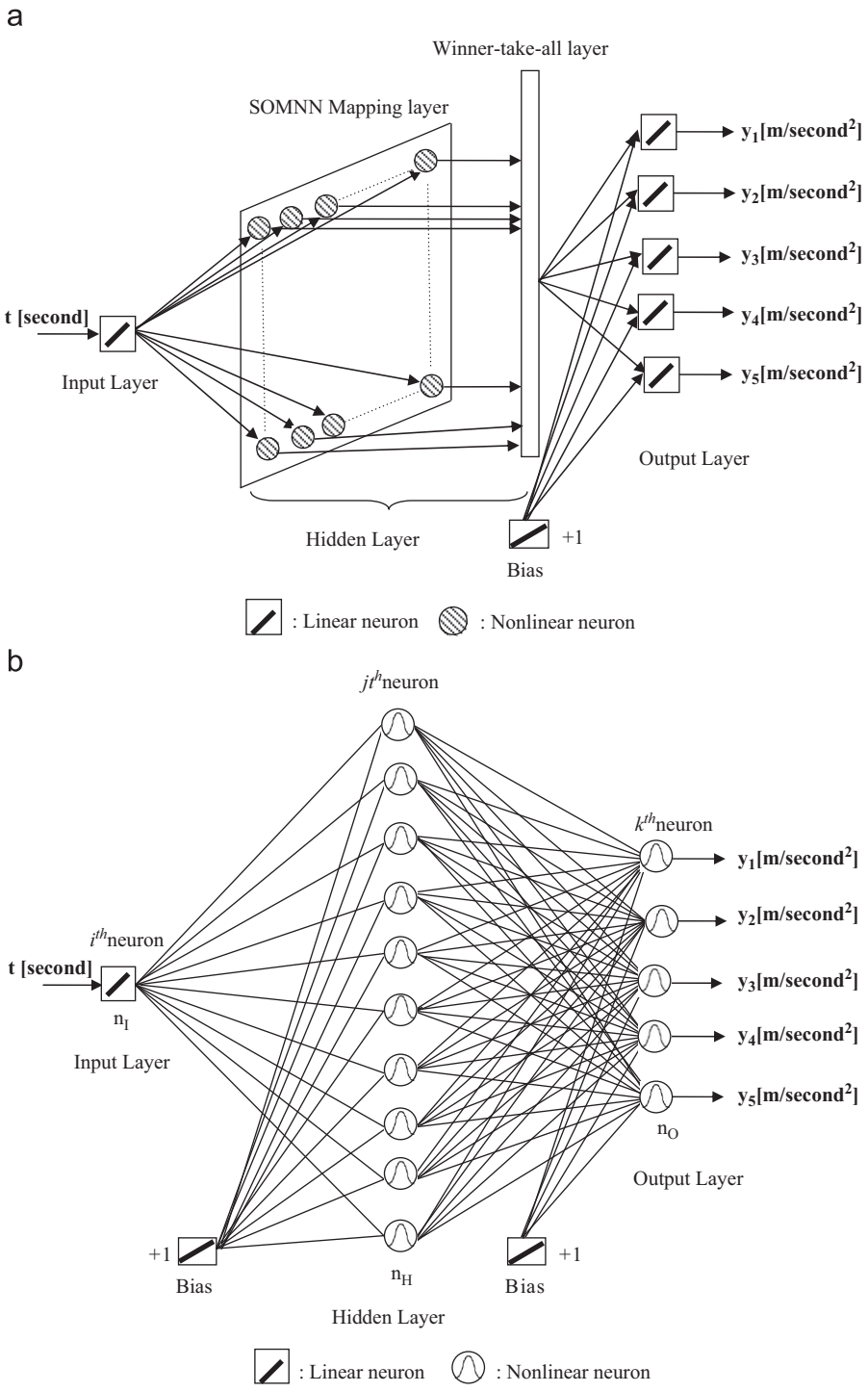

Fig. 5. (a). Schematic representations of the SOMNN analyzer and (b). Schematic representations of the RBNN analyzer.

The output signal of hidden layer of the proposed neural network, i.e., acceleration of the welding robot manipulator's joints, can be described in the following equations:

$$m_j(t) = f\left(\sum_{j=1}^{10} w_{ij}(t)t + b_j\right) \tag{5}$$

where $m_j(t)$ is the output of the jth neuron in the hidden layer, w_{ij} is the weight of the connection between the input layer neurons and the hidden layer neurons, b_j is the bias of the jth neuron in the hidden layer. b_j can be regarded as the weight of the connection between a fixed input of unit value and neuron j in the hidden layer. The activation function which is used as sigmoid function of the hidden layer

$$f(t) = \frac{1}{1+e^{-t}} \tag{6}$$

The output signal of the hidden layer can be rearranged in the following form:

$$m_j(t) = \frac{1}{1+e^{-\left(\sum_{j=1}^{10} w_{ij}(t)t + b_j\right)}} \tag{7}$$

The output signal of the output layer of the proposed neural network can be expressed in the following form:

$$y_k(t) = g\left(\sum_{j=1}^{10}\sum_{k=1}^{5} w_{jk}(t)m_j(t) + b_k\right) \tag{8}$$

where $g(t)$ is activation functions of the output layer and can be described as follows:

$$g(t) = t \tag{9}$$

The output signal of the output layer can be written by

$$y_k(t) = \sum_{k=1}^{5}\left[\frac{1}{1+e^{-\left(\sum_{j=1}^{10} w_{ij}(t)t + b_j\right)}}\right] w_{jk}(t) + b_k \tag{10}$$

where w_{jk} are the weights between jth neurons hidden layer and kth neurons output layer and b_k is the bias of the kth neurons in the output layer. Two learning methods, which are used to analyze accelerations of the welding robot manipulator's joints, are briefly described in the following subsections.

3.1. Self organizing map neural network (SOMNN)

SOMNN consists of a regular, usually two-dimensional, grid of map units. Each unit is represented by a prototype vector, where input vector is dimension. The units are connected to adjacent ones by a neighborhood relation. The number of map units, which typically varies from a few dozen up to several thousand, determines the accuracy and generalization capability of the SOMNN. Data points lying near each other in the input space are mapped onto nearby map units. Thus, the SOMNN can be interpreted as a topology preserving mapping from input space onto the 2-D grid of map units. The SOMNN is trained iteratively. At each training step, a sample vector z is randomly chosen from the input data set. Distances between z and all the prototype vectors are computed. The best matching unit, which is denoted here by b, is the map unit with prototype closest to z

$$\|z - m_b\| = \min_i\{\|z - m_i\|\} \tag{11}$$

The update rule for the prototype vector of unit i is

$$m_i(t+1) = m_i(t) + \alpha(t)h_{bi}(t)[z - m_i(t)] \tag{12}$$

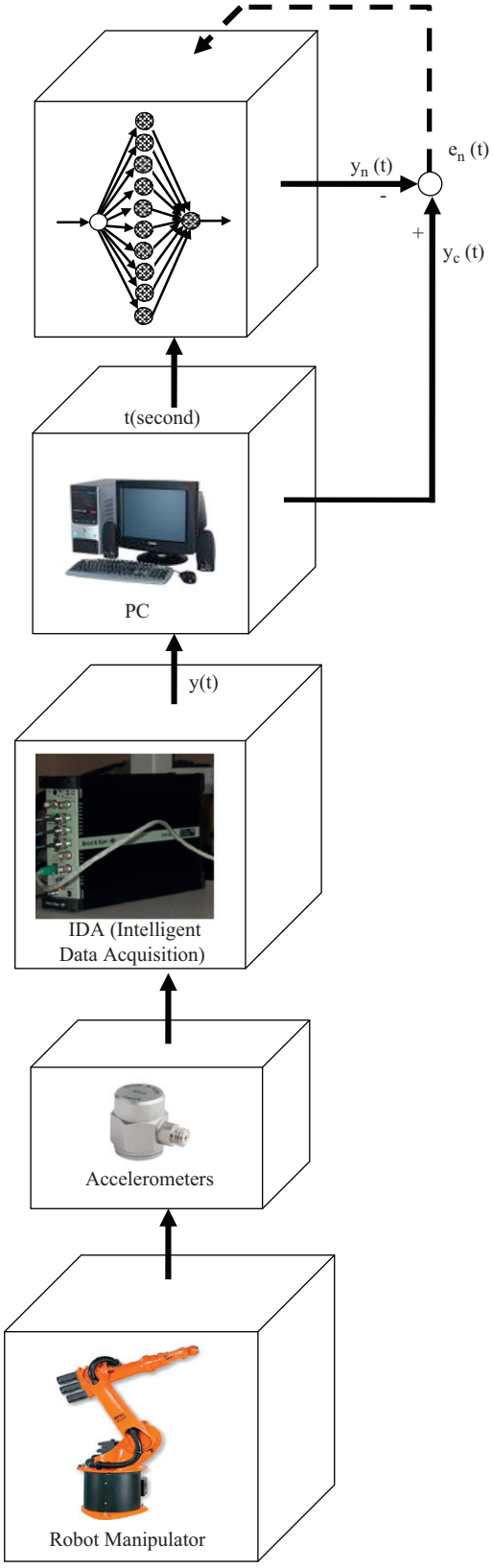

Fig. 6. Flow chart of experimental setup.

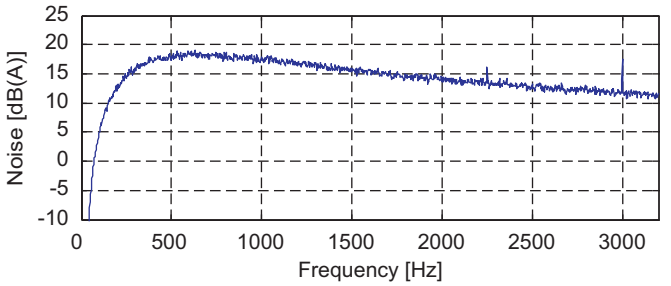

Fig. 7. Noise variation of the welding robot manipulator with 1 rpm running speed.

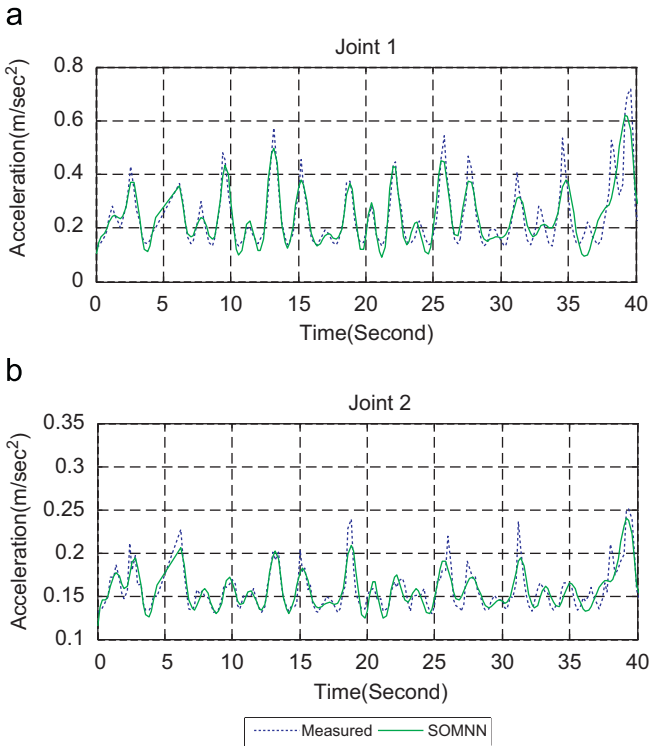

Fig. 8. Acceleration variations of the welding robot manipulator joints 1 and 2 with 1 rpm running speed, using the SOMNN structure.

where $\alpha(t)$ is an adaptation coefficient, $h_{bi}(t)$ is the neighborhood kernel centered on the winner unit.

$$h_{bi}(t) = \exp\left(-\frac{\|r_b - r_i\|^2}{2\sigma^2(t)}\right) \tag{13}$$

where r_b and r_i are positions of neurons b and i on the SOMNN grid. Both $\alpha(t)$ and $\sigma(t)$ decrease monotonically with time. In the case of a discrete data set and fixed neighborhood kernel, the errors function of SOMN is as follows:

$$E = \sum_{i=1}^{N}\sum_{j=1}^{M} h_{bj}\|z_i - m_j\|^2 \tag{14}$$

where N is number of training samples and M is the number of map units. Neighborhood kernel h_{bj} is centered at unit b, which is the best matching unit of vector z_i, and evaluated for unit j [15].

3.2. Radial basis neural network (RBNN)

Radial basis neural network (RBNN) is feedforward and has only one hidden layer. The RBNN structure is good at modeling nonlinear data and can be trained in one stage rather than using an iterative process as in multi-layer perception neural network and also learn the given application quickly. They are useful in solving problems, where the input data are corrupted with additive noise.

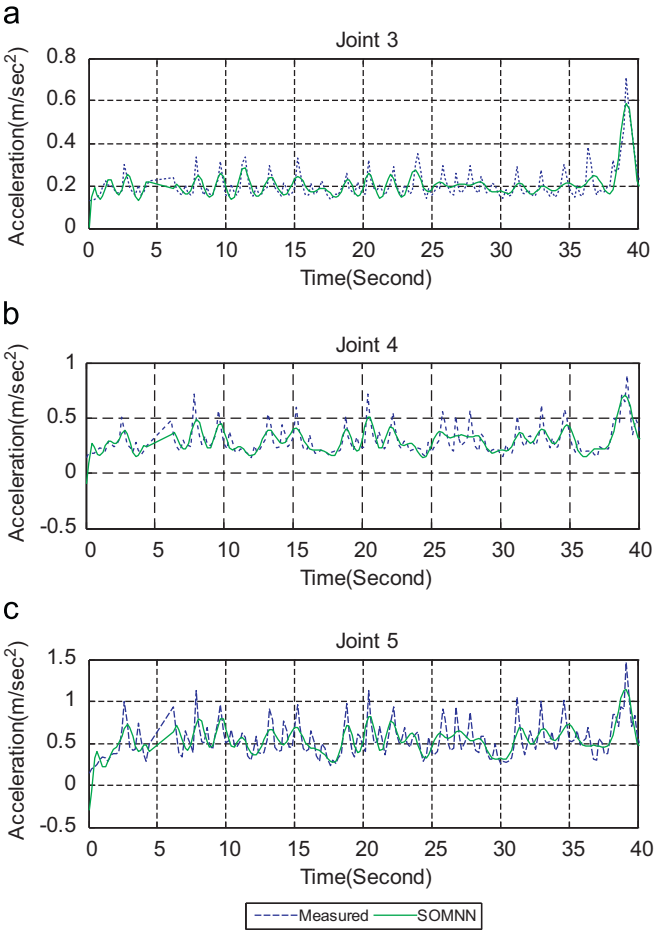

Fig. 9. Acceleration variations of the welding robot manipulator joints 3, 4 and 5 with 1 rpm running speed, using the SOMNN structure.

The transformation functions used are based on a Gaussian distribution. If the error of the network is minimized appropriately, it will produce outputs that sum to unity, which will represent a probability for the outputs. The RBNN structure has an input layer, a hidden layer of radial units and an output layer of linear units. The RBNN model is mathematically represented as follows:

$$f(x) = \sum_{i=1}^{n} w_i \phi(\|x - x_i\|) + \sum_{j=1}^{m} c_j p_j(x) \tag{15}$$

where n is the number of sampling points, x is the vector of input variables, x_i is the center of basis function ϕ, w_i is the unknown weighting coefficient, m is the total number of terms in the polynomial and c_j is the corresponding coefficient. Therefore, an RBNN is actually a linear combination of n basis functions with weighted coefficients. In this study, Gaussian basis function is used as follows:

$$\phi(t) = e^{-ct^2}, \quad 0 < c \le 1 \tag{16}$$

4. Experimental and simulation analyses

Experimental and simulation investigation on robot manipulator's fault detection has been carried out in two stages. First

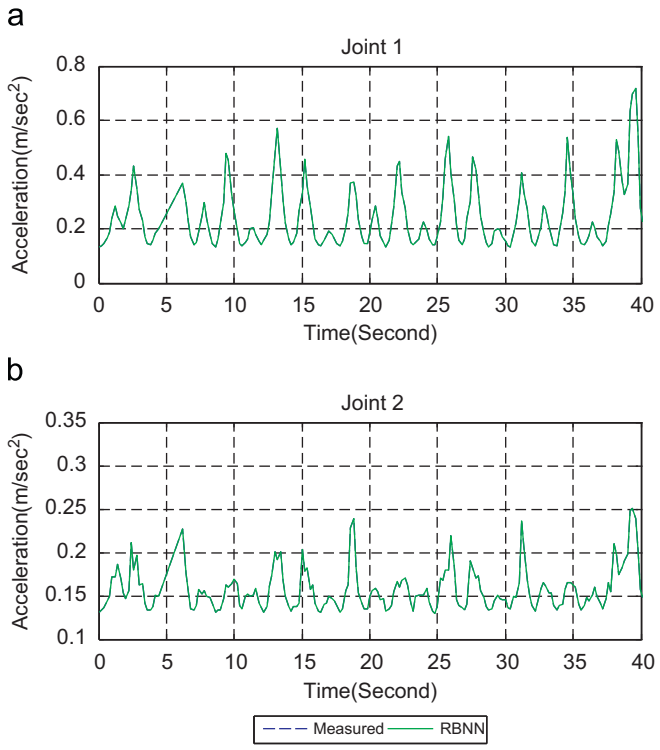

Fig. 10. Acceleration variations of the welding robot manipulator joints 1 and 2 with 1 rpm running speed, using an RBNN structure.

stage is experimental measurements on robot manipulator's joints. The process consists of an intelligent data acquisition (IDA), 5 accelerometers, a microphone and PC. The experimental setup, used to collect the joint accelerations for the case of the two different running speeds of welding robot manipulator, is given in Fig. 6. On the second stage, the measured experimental accelerations values are used as desired signals of neural networks. Neural networks are tested to predict exact signals of robot manipulator's joints with two types of learning algorithms.

The setup used for the experiments and a schematic diagram are represented in Fig. 6. Experimental and simulation results are shown in Figs. 7–16, respectively. By considering the 1 rpm running speed, the experimental noise variation of the welding robot manipulator is given in Fig. 7. Figs. 8 and 9 present the acceleration results of the desired SOMNN approach and experimental results of the welding robot manipulator joints with 1 rpm running speeds for the desired trajectory. It is clear to see from graphs; that there are differences between experimental and the SOMNN results for both cases. In particular, these differences occur at the peak values of the experimental measurements.

The other type of neural network, i.e., the RBNN structure is used to predict acceleration variations of the welding robot manipulator joints with 1 rpm running speed and the results are shown in Figs. 10 and 11. As seen in relevant figures, the RBNN approach is robust stable to analyze the vibration parameters of such welding robot manipulator joints for different prescribed and joint speeds.

Furthermore, Fig. 12 shows noise variation of the welding robot manipulator for the case of 2 rpm running speed. The noise variations for 1 and 2 rpm are evaluated together; the main factor is not the robot. The system equipments such as control panel, etc. are very effective on the noise generation. Figs. 13 and 14 indicate the results of experimental and SOMNN approach for

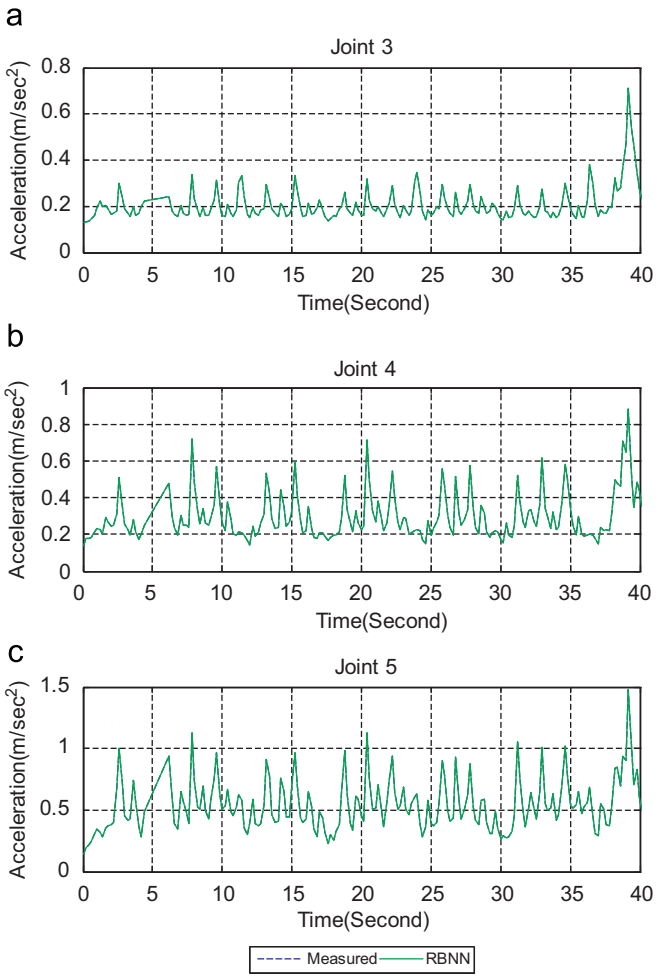

Fig. 11. Acceleration variations of the welding robot manipulator joints 3, 4 and 5 with 1 rpm running speed, using an RBNN structure.

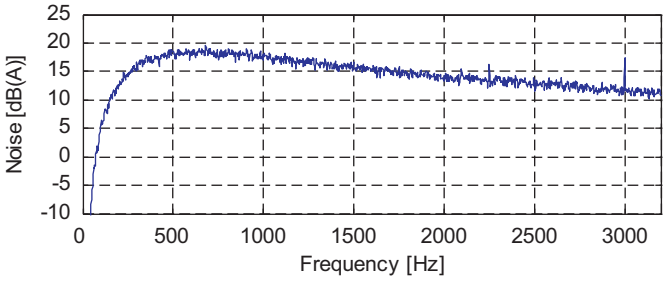

Fig. 12. Noise variation of the welding robot manipulator with 2 rpm running speed.

acceleration variations of the welding robot manipulator joints with 2 rpm running speed. As pointed out from the figures, the results of SOMNN approach give poor performance. Again, the RBNN structure is used to predict acceleration of the welding robot manipulator joints with 2 rpm running speed (see Figs. 15 and 16). Also, Table 2 shows structural, training parameters and root mean square errors (RMSEs) of neural networks. It is clear to see from figures and Table 2, the proposed RBNN approach has superior performance for predicting accelerations variation of the welding robot manipulator joints for different running speeds.

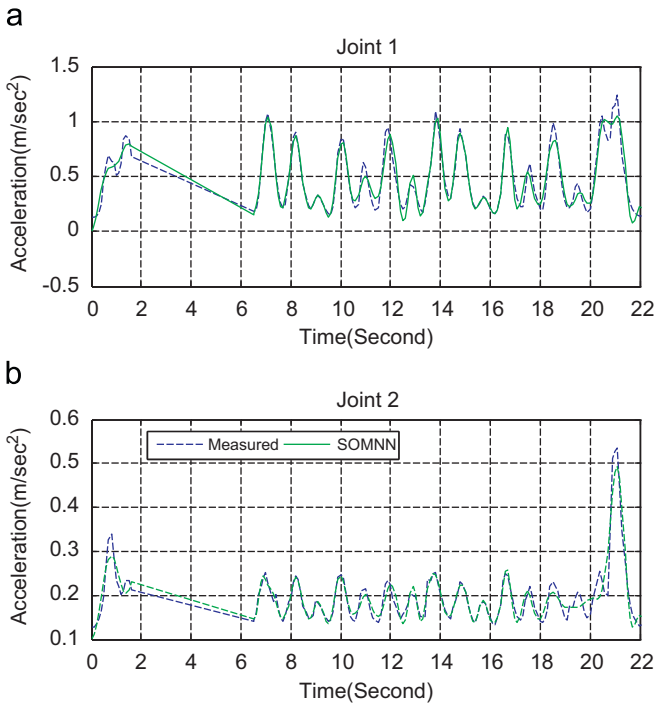

Fig. 13. Acceleration variations of the welding robot manipulator joints 1 and 2 with 2 rpm running speed, using the SOMNN structure.

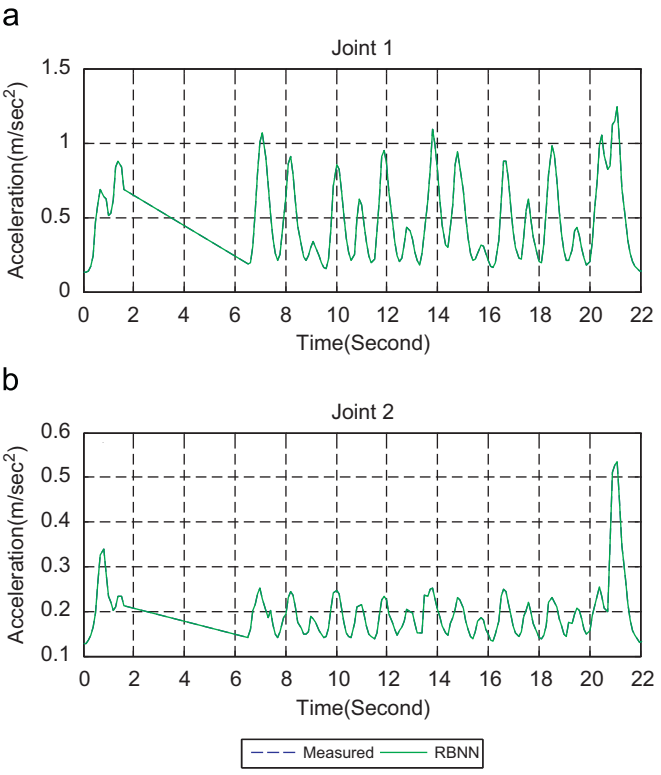

Fig. 15. Acceleration variations of the welding robot manipulator joints 1 and 2 with 2 rpm running speed, using an RBNN structure.

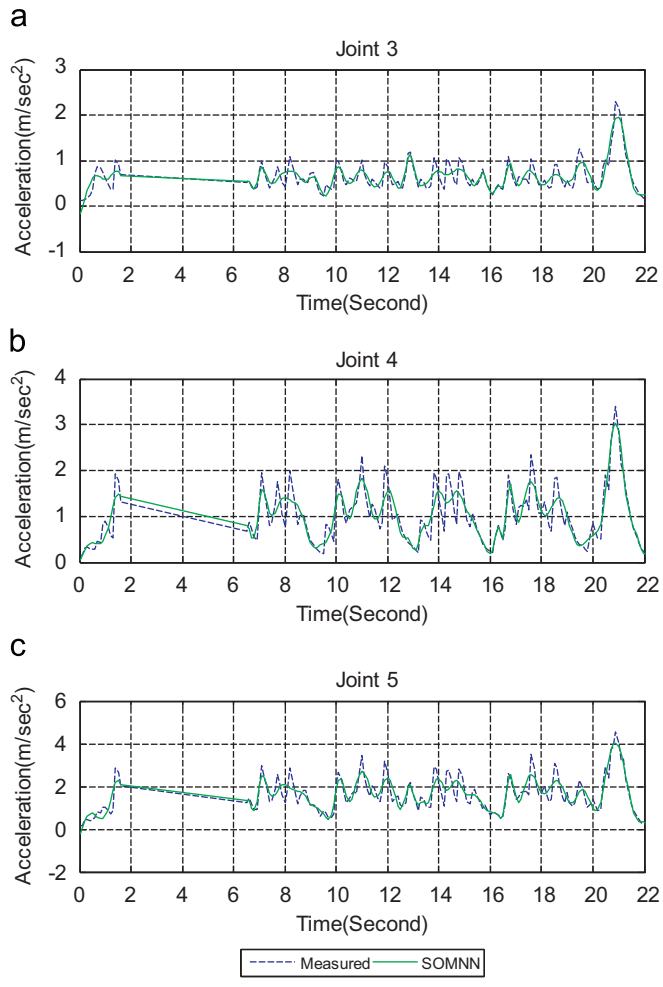

Fig. 14. Acceleration variations of the welding robot manipulator joints 3, 4 and 5 with 2 rpm running speed, using the SOMNN structure.

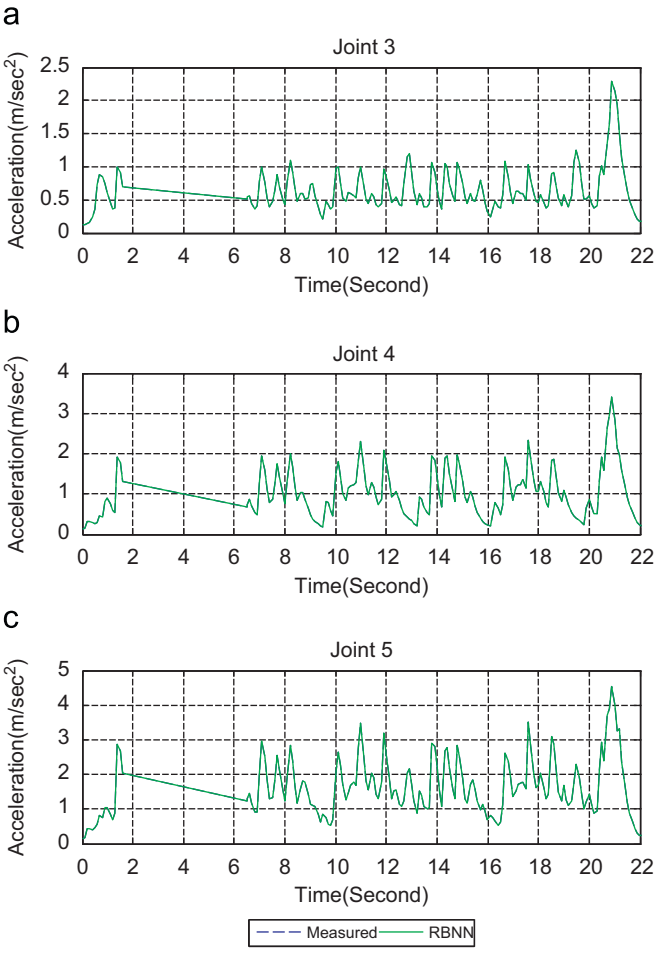

Fig. 16. Acceleration variations of the welding robot manipulator joints 3, 4 and 5 with 2 rpm running speed, using an RBNN structure.

Table 2
Structural and training parameters of the feedforward neural networks with two learning algorithms.

Running speed of end-effectors	NN type	η	γ	N	n_I	n_H	n_O	RMSEs
1 rpm	SOMNN	0.4	0.5	400,000,000	1	10	5	0.0600
1 rpm	RBNN	0.4	0.5	400,000,000	1	10	5	**0.0004**
2 rpm	SOMNN	0.4	0.5	400,000,000	1	10	5	0.0439
2 rpm	RBNN	0.4	0.5	400,000,000	1	10	5	**0.0004**

5. Conclusion and discussion

In this study, fault detection based neural network for an experimental industrial welding robot has been implemented. Joint accelerations of robot are considered as evaluation criteria. For this purpose, an experimental setup is used to collect the related values. The accelerations of welding robot, which has six degrees of freedom, are analyzed. In order to design an optimal neural estimator, two types of neural networks are used for comparingeach other. The results obtained for both the running speeds show that the proposed RBNN has a robust stability to analyze the accelerations of manipulator joints during a prescribed trajectory. The major advantage of an RBNN uses Gaussian function, gives a response that drops off rapidly as the distance between the hidden unit and the input vector increases and is symmetrical about the radial axis. It has been scientifically proved that the RBNN structure is given the best approach rather than other structure.

The proposed neural network based fault detection technique could be employed to predict fault isolation of robot manipulator joints in considering with a larger number of degrees of freedom.

References

[1] Caccavale F, Cilibrizzi P, Pierri F, Villani L. Actuators fault diagnosis for robot manipulators with uncertain model. Control Engineering Practice 2009;17:146–157.
[2] Halder B, Sarkar N, Analysis of order of redundancy relation for robust actuator fault detection, Control Engineering Practice 2009;17:966–73.
[3] Jing Z, Cheng F. On the joint velocity jump during fault tolerant operations for manipulators with multiple degrees of redundancy. Mechanism and Machine Theory 2009;44:1201–10.
[4] Siqueira AAG, Terra MH, Buosi C. Fault-tolerant robot manipulators based on output-feedback H∞ controllers. Robotics and Autonomous Systems 2007;55:785–94.
[5] Hassan M, Notash L. Optimizing fault tolerance to joint jam in the design of parallel robot manipulator. Mechanism and Machine Theory 2007;42:1401–1417.
[6] Hassan M, Notash L. Design modification of parallel manipulators for optimum fault tolerance to joint jam. Mechanism and Machine Theory 2005;40:559–77.
[7] Tinós R, Terra MH, Bergerman M. A fault tolerance framework for cooperative robotic manipulators. Control Engineering Practice 2007;15:615–25.
[8] Yasuda T, Ohkura K, Ueda K. A homogeneous mobile robot team that is fault-tolerant. Advanced Engineering Informatics 2006;20:301–11.
[9] Verma V, Simmons R. Scalable robot fault detection and identification. Robotics and Autonomous Systems 2006;54:184–91.
[10] Jing Z, Kailiang Z, Xuebin Y. Study on fault tolerant workspace and fault tolerant planning algorithm based on optimal initial position for two spatial coordinating manipulators. Mechanism and Machine Theory 2006;41:584–95.
[11] Notash L, Huang L. On the design of fault tolerant parallel manipulators. Mechanism and Machine Theory 2003;38:85–101.
[12] Yang JM. Tripod gaits for fault tolerance of hexapod walking machines with a locked joint failure. Robotics and Autonomous Systems 2005;52:180–9.
[13] Jing Z, Xuebin Y, Lei Z. The optimization of initial posture with avoidance of the sudden change in joint velocity for fault tolerant operations of two coordinating redundant manipulators. Mechanism and Machine Theory 2005;40:659–68.
[14] Liu H, Coghill GM. A model-based approach to robot fault diagnosis. Knowledge-Based Systems 2005;18:225–33.
[15] Vesanto J, Alhoniemi E. Clustering of the Self-Organizing Map. IEEE Transactions on Neural Networks 2000;11:586–600.